JOURNAL OF MATERIALS SCIENCE 21 (1986) 1187–1205

The elastic constants and structure of the vitreous system Mo–P–O

B. BRIDGE, N.D. PATEL*
Department of Physics, Brunel University, Kingston Lane, Uxbridge, Middlesex UB8 3PH, UK

The preparation of glasses with compositions spanning the entire vitreous range obtainable from melting phosphorous pentoxide with molybdenum trioxide, and phosphoric acid with ammonium molybdate, in open crucibles, is described. The second order elastic constants of these Mo–P–O glass systems have been obtained from ultrasonic wave velocity measurements. The most striking features of the results are two discontinuities in the compositional gradient of each elastic modulus, at compositions of ~53 and 63 mol% MoO_3 content. These compositions approximate to those of molybdenum metaphosphate and molybdenum pyrophosphate crystals. A second noteworthy feature is that the elastic moduli display a substantial overall increase with molybdenum content, 36% for bulk and 83% for shear over the entire composition range, even though the Mo–O bond stretching force constant is less than half that of the P–O bond. A detailed qualitative interpretation of these features is made, in terms of the proposed compositional dependence of the crosslink densities of the molybdenum and phosphorus atoms, and the atomic ring sizes.

1. Introduction

the Mo–P–O system is interesting in that it forms water-soluble, but otherwise stable, glasses over a wide and continuous compositional range of 0 to ~83 mol% MoO content. Ultrasonically determined elastic moduli data can be a useful method of monitoring structural changes in binary glass systems. With ultrasonic propagation, bulk properties can be measured, and are relatively little affected by what is happening near the specimen surfaces, whereas many other analytical methods (X-ray, electron microscopy, infrared spectroscopy, etc.) either require specimens in powdered form or permit only surface examination, so that water absorption severely affects their efficiency in the characterization of phosphate glasses. In this paper, preparation of the entire range of Mo–O–P glass compositions that can be obtained by melting together MoO_3 and P_2O_5, and also ammonium molybdate with orthophosphoric acid, in open crucibles, is described. The composition range, covering 0 to 83 mol% MoO_3 content, is perhaps the widest known for binary mixtures of a glassformer with another oxide which does not form glasses by itself. The second-order elastic constants of the two glass systems have been determined from ultrasonic wave velocity measurements, and are found to display a striking compositional dependence, the gradient of each constant undergoing three changes of sign. The results are interpreted rather convincingly on the assumption that the glasses consist of a disordered arrangement of the basic oxides together with meta, ortho, and pyrophosphate groups in proportions which depend upon the Mo^{5+} and Mo^{6+} contents in the glasses as determined by chemical analysis [1].

2. Review of existing data on the structure and properties of molybdenum glasses

Perhaps the first report on the formation of glasses in the system MoO_3–P_2O_5 was by Schulz [2] and followed by Baynton *et al.* [3]. According to Schulz the glasses were dark in colour and during the formation of these glasses, there was some loss of oxygen. From conductivity measurements, it was confirmed that the metal atoms (i.e. the molybdenum atoms) were partly reduced, which conclusion was supported by quantitative measurement of the degree of reduction. By means of paper chromatography, Kierkegaard [4] studied Mo–P–O glasses made from ammonium molybdate and orthophosphoric acid, and anhydrous MoO_3 and P_2O_5, together with glasses prepared from the melts of the crystalline phases, i.e. $MoOPO_4$, $MoO_{3-x}P_2O_5$, $Mo(OH)_3PO_4$ $MoO_2(PO_3)_2$ and $(MoO_2)_2P_2O_7$. The glasses prepared from anhydrous molybdenum trioxide show a minimum degree of condensation of the phosphate tetrahedra. Thus the highest value of n in $P_nO_{(3n+1)}^{(n+2)-}$ was found to increase roughly linearly as the MoO_3 content in the glasses decreases, i.e. the number of different phosphate groups decreases with increasing amounts of MoO_3 [4] (see Table I, and Fig. 1). This trend seems to be consistent with the behaviour of the viscosity, i.e. the viscosity decreases monotonically with increasing amount of MoO_3. The value of x in the composition $MoO_{3-x} \cdot yP_2O_5$ for molybdenum phosphate glasses, was found to be a maximum at 50 mol% MoO_3, i.e. $y = 1$, the range at which the solubility in hot water is minimum. This property has been related to a higher degree of reduction of the molybdenum

Present address: Department of Metallurgy and Materials Science, MacMaster University, Hamilton, Ontario L85 4L7, Canada.

0022–2461/86 $03.00 + .12

TABLE I Data assembled from [4, 7, 10, 11] for MoO_3–P_2O_5 crystalline compounds and corresponding glasses, i.e. glasses obtained by melting these crystals

Crystalline compound	Density ($g\,cm^{-3}$)	Composition calculated (mol %)		Molar volume (cm^3)	Corresponding glass no.
		MoO_3	P_2O_5		
$MoOPO_4$	4.06	66.7	33.3	35.43	G_1
$MoO_{\sim 2.5} \cdot P_2O_5$		50.2	49.8		G_2
$MoO_2(PO_3)_2$	3.37	49.8	50.2	42.42	G_3
$Mo(OH)_3PO_4$	2.82	59.4	29.8		G_4
$(MoO_2)_2P_2O_7$	3.44	66.5	33.5	41.65	G_5
Corresponding glasses					
G_1	3.36	69.5	30.5	42.66	
G_2	3.01	51.9	48.1	47.50	
G_3	2.99	53.1	46.9	47.83	
G_4	3.28	67.2	32.8	43.68	
G_5	3.10	67.3	32.7	46.22	

atoms [2, 4], since more reduced glasses prepared from ammonium molybdate and orthophosphoric acid, show very low solubility in hot water.

Molybdenum may be present in the following states of oxidation: Mo^{6+}, Mo^{5+}, Mo^{4+} and Mo^{3+}, which may be relatively stable as there exist many relatively stable oxidation states in second row transition elements [5, 6]. Under proper conditions only, the molybdenum ions will be reduced to a lower valence state to give the intensely coloured "heteropoly blue". The blue reduction product has variable composition and its constitution is uncertain. Apparently both Mo^{6+} and Mo^{5+} elements are present. The heteropoly–molybdic acids are formed when the molybdate reacts in acid solution with phosphate, arsenate, germanate and silicate.

3. Relationship between Mo–P–O glasses and crystalline phases or the Mo–P–O system

In the Mo–P–O system, vitreous states are possible for all quantities of $MoO_3 < 86$ mol %. In addition, the crystals $Mo(OH)_3PO_4$ [7], $MoO_2(PO_3)_2$ [8], $(MoO_2)_2P_2O_7$ [9], and $MoOPO_4$ [10] are known to exist and have been studied by means of X-ray methods, yet little is known regarding a crystal structure, which forms at about 86.5 mol % MoO_3, and a green crystalline substance in the form of $MoO_{3-x} \cdot P_2O_5$ [4] (where $x \sim 0.5$, the composition corresponding to metaphosphate).

The compositions and density of these crystalline phases are given in Table I, together with data on their glassy analogues, i.e. glasses which are prepared by melting these crystals. The chromatograms for Mo–P–O crystals and glasses sketched in Figs. 1a and b show that generally the crystals display fewer phosphate groups than their vitreous analogues.

For the interpretation of the elastic behaviour of the Mo–P–O vitreous system that we are to present, an understanding of the crystal structures mentioned above, is essential. Amongst other things, the interpretation requires an assumption of how the co-ordination numbers and crosslink densities of the molybdenum and phosphorus atoms change with composition. Direct information of this type (from EXAFS* measurements for example) is not presently available nor can it be guaranteed to be obtainable. Our alternative has been to assume that in a glass, structural groupings similar to those of the end-member oxides, and meta, ortho, and pyrophosphate crystals, occur in mole fractions which are determined by the glass composition (in mol % MoO_3). It should be emphasized that this is not necessarily a phase separation model, for we envisage that the structural elements which resemble one crystalline phase or another could consist of only a few PO_4 tetrahedra and/or MoO_6 octahedra. There will, of course, be a distribution of bond angles between the polyhedra instead of the fixed values obtaining in the crystals and they will be three-dimensionally connected even though some of the crystalline forms concerned are layer structures. It will be convenient to give a brief description of the crystalline phases involved for otherwise at least six different publications would have to be consulted to follow our interpretation.

3.1. P_2O_5 ([11] p. 684)

There are three forms which represent different ways of linking together tetrahedral PO_4 groups by the sharing of three corners to form (a) P_4O_{10} molecules, (b) a layer structure of P_6O_6 rings, and (c) a three-dimensional network of $P_{10}O_{10}$ rings. Only the latter two are of interest to us as we do not envisage the presence of molecular units in glass.

3.2. MoO_3 ([11] pp. 439, 473)

MoO_6 octahedra share two adjacent edges with two other octahedra and in a perpendicular direction the octahedra share vertices with two other octahedra, to form a layer. Thus three oxygen atoms of each octahedron are bonded to three molybdenum atoms, two others are bonded to two molybdenum atoms, whilst the sixth atom is unshared, with the layers held together by Van der Waals forces. Thus in a plane containing the shared edges, the structure consists of corrugated chains of interconnected Mo_2O_2 rings; whilst in a perpendicular direction, vertex sharing leads to a layer of Mo_4O_4 rings.

3.3. Molybdebum metaphosphate $MoO_2(PO_3)_2$ [8]

Tetrahedral PO_4 groups share two corners with other PO_4 tetrahedra to give continuous PO_3 chains orientated with the chain axes parallel to the *c*-axis. The molybdenum atoms are situated between the chains so that each of the metal atoms is coordinated by six oxygen atoms in an octahedral arrangement. Four of these oxygens are shared with the PO_4 groups, i.e. each MoO_6 octahedra shares four corners with the PO_4 groups to produce infinite wave-like layers of the composition $(MoO_2(PO_3)_2)_n$. However, the other two oxygen atoms in every octahedron are bonded to only one molybdenum atom so that the crystals are built up of

*Extra fine structure X-ray diffraction techniques.

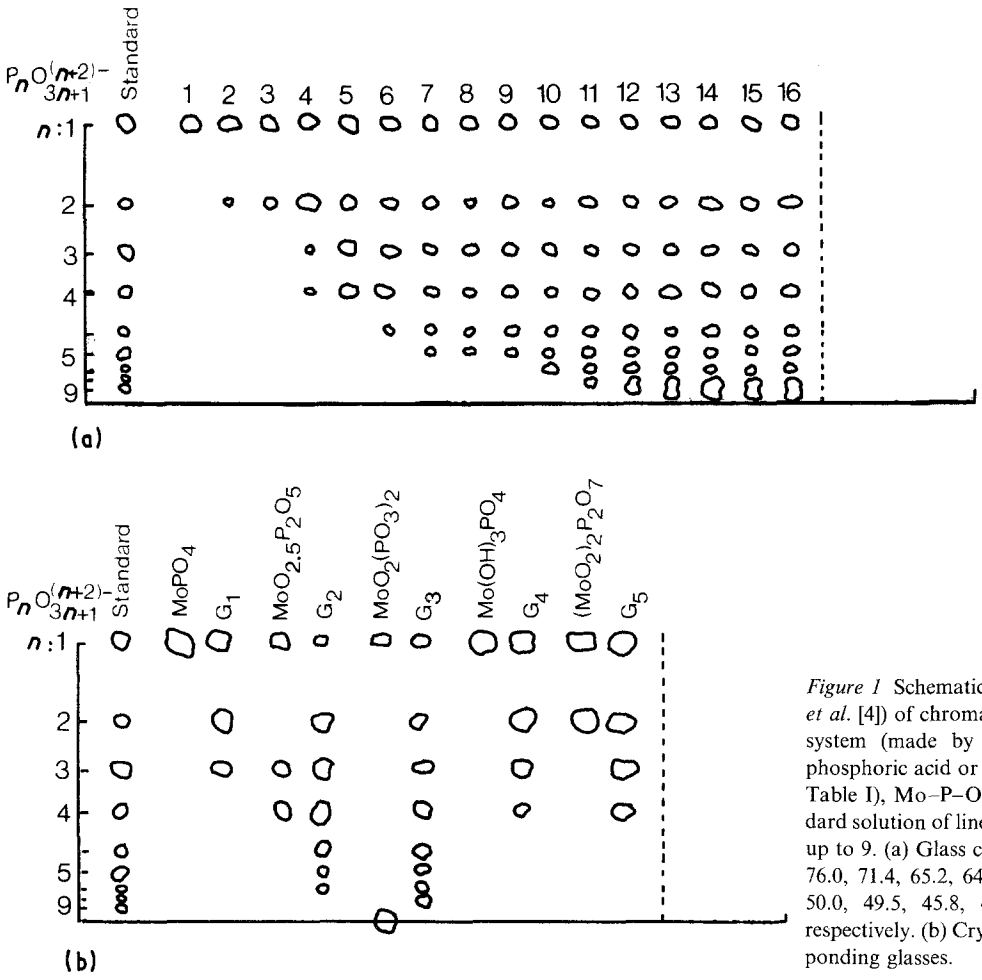

Figure 1 Schematic drawings (after Kierkegaard *et al.* [4]) of chromatograms of the Mo–P–O glass system (made by melting together MoO_3 with phosphoric acid or by melting the crystals listed in Table I), Mo–P–O crystalline phases, and a standard solution of linear phosphates $P_nO_{3n+1}^{(n+2)-}$ with n up to 9. (a) Glass compositions (1 to 16), 86, 81.5, 76.0, 71.4, 65.2, 64.2, 61.7, 65.0, 63.9, 50.7, 50.3, 50.0, 49.5, 45.8, 40.1, and 37.1 mol% MoO_3, respectively. (b) Crystalline compounds and corresponding glasses.

layers held together by Van de Waals forces. Each octahedron shares corners with two tetrahedra which also share edges with each other (i.e. they are adjacent members of the same chain of tetrahedra), to produce a chain of separate MoP_2O_3 rings linked together by oxygen atoms, along every chain. The other two shared corners of each octahedron involve separate PO_3 chains so that each MoP_2O_3 ring is interconnected with two other PO_3 chains via two $Mo_2P_2O_4$ rings. In this way corrugated chains of alternating MoP_2O_3 and $Mo_2P_2O_4$ rings are produced, which are, in turn, linked together into a double layer by two layers of $Mo_2P_6O_8$ rings.

3.4. Molybdenum pyrophosphate $(MoO_2)P_2O_7$ [9]

MoO_6 octahedra share corners with two other MoO_6 octahedra to form infinite chains. These chains are linked into a three-dimensional network by P_2O_7 groups (i.e. by pairs of PO_4 tetrahedra which have a common oxygen). Each P_2O_7 group shares corners with six MoO_3 octahedra in three chains (two octahedra being in each chain). Each octahedra thus shares three corners (i.e. three oxygens) with three P_2O_7 groups, and two oxygens are shared with neighbouring octahedra, leaving a sixth oxygen bonded to only a single molybdenum atom. Since every P_2O_7 group shares two edges with two octahedra which also share an edge with each other, this structure may be described as a three-dimensional network of interconnected $Mo_2P_2O_4$ rings.

3.5. Molybdenum orthophosphate $MoOPO_4$ [10]

Distorted octahedral M_6O_6 groups share two corners with two other octahedra to form infinite chains parallel to the c-axis. The chains are then coupled together by PO_4 groups, so that every MoO_6 octahedron shares corners with four phosphate tetrahedra, each one of which shares corners with four octahedra, to give a three-dimensional network. Of the six oxygen atoms coordinating with each molybdenum atom, four are bonded to two molybdenum, thus unlike the pyrophosphate and metaphosphate structures, there are no oxygen atoms bonded to only one molybdenum atom in this crystal. As the distortion of the octahedra is so pronounced it has been argued that it is more appropriate to describe the structure in terms of five coordination. Such structural details, however, do not materially alter our qualitative interpretation of data. Viewed in a direction perpendicular to the chain axes, two adjacent octahedra in one chain are linked via two tetrahedra, to two adjacent octahedra of another chain, producing layers of interconnected $Mo_4P_2O_6$ rings. Viewed along the chain axes pairs of tetrahedra share edges with the same pair of octahedra, so that layers of interconnected $Mo_2P_2O_4$ rings are seen.

For our qualitative interpretation of the elastic constants of Mo–P–O glasses, the important quantities in respect of the above crystals are the numbers of network bonds and crosslink densities in the formula unit for each type of cation, and the atomic ring sizes, i.e. the shortest closed circuits of the network bonds.

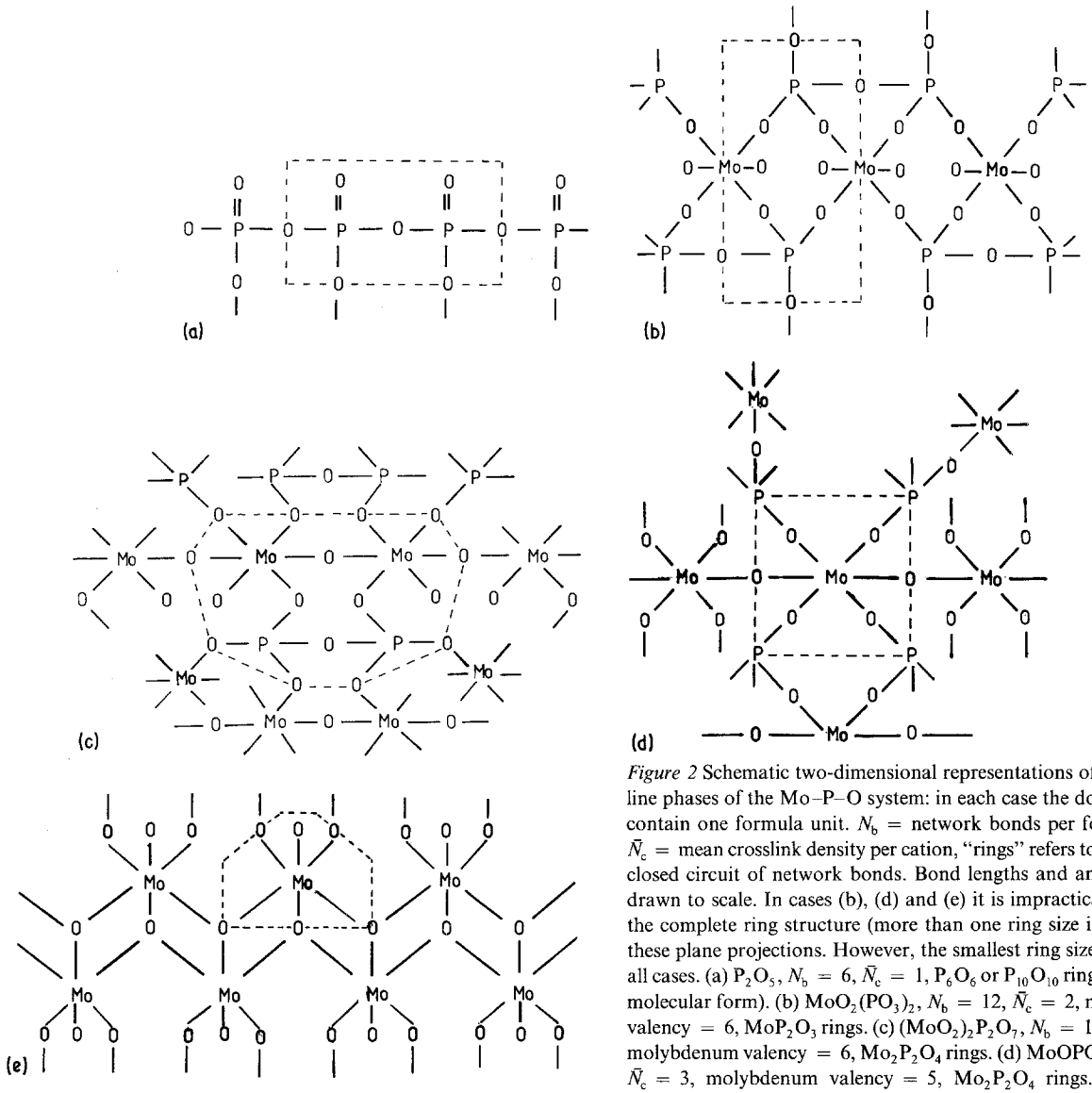

Figure 2 Schematic two-dimensional representations of the crystalline phases of the Mo–P–O system: in each case the dotted regions contain one formula unit. N_b = network bonds per formula unit, $\bar{N}_c$ = mean crosslink density per cation, "rings" refers to the shortest closed circuit of network bonds. Bond lengths and angles are not drawn to scale. In cases (b), (d) and (e) it is impractical to display the complete ring structure (more than one ring size is present) in these plane projections. However, the smallest ring size is shown in all cases. (a) P_2O_5, $N_b = 6$, $\bar{N}_c = 1$, P_6O_6 or $P_{10}O_{10}$ rings (excluding molecular form). (b) $MoO_2(PO_3)_2$, $N_b = 12$, $\bar{N}_c = 2$, molybdenum valency = 6, MoP_2O_3 rings. (c) $(MoO_2)_2P_2O_7$, $N_b = 18$, $\bar{N}_c = 2.5$, molybdenum valency = 6, $Mo_2P_2O_4$ rings. (d) $MoOPO_4$, $N_b = 10$, $\bar{N}_c = 3$, molybdenum valency = 5, $Mo_2P_2O_4$ rings. (e) MoO_3, $N_b = 5$, $\bar{N}_c = 3$, molybdenum valency = 6, Mo_2O_2 rings.

Bond lengths and relative orientations are not to be considered. The above quantities of interest are most easily identified by drawing two-dimensional representations of each crystal type based on the above structural descriptions (Figs. 2a to e). In all the crystals containing molybdenum, except the pyrophosphate, there are two or more atomic ring sizes present and it is not possible to display clearly the complete pattern of ring structures in these two-dimensional projections. However, in all cases, the smallest ring size, particularly relevant to our present discussion, is clearly identified.

4. Preparation of Mo–P–O glasses

4.1. Glasses prepared from anhydrous molybdenum trioxide and phosphorous pentoxide

Molybdenum–phosphate glasses were prepared from dry mixtures of anhydrous molybdenum trioxide (Analar reagent grade, molecular weight = 143.94, BDH Ltd) and phosphorous pentoxide (Analar reagent grade, molecular weight = 141.95, BDH Ltd). Quantities of MoO_3 and P_2O_5 amounting to 72 g, were mixed together in various proportions in the range 5 to 85 mol % MoO_3 in alumina crucibles (capacity 100 g). These mixes were placed in an electrically heated furnace held between 900 and 1200° C, the highest temperature being applicable to the mixes in which MoO_3 amounts ranged from 35 to 60 mol %. The melt was equilibrated at the melt temperature for about 20 min with frequent stirring with an alumina rod, to ensure homogeneous melts. Glasses containing below 50 mol% MoO_3 (starting composition) where covered with an alumina lid, in order to minimize the loss of P_2O_5.

Then the melts were cast into stainless steel split moulds of cylindrical section, which were previously heated in an annealing furnace held at the tempeature at which the glass produced was subsequently to be annealed, in order to minimize the thermal stress in the solidified melts. Typically, three to four glass rods were obtained from each melt, each of length ~ 1 cm and diameter either 1 or 1.6 cm.

4.2. Glasses prepared from orthophosphoric acid and ammonium molybdate

Another series of Mo–P–O glasses (more reduced glasses) was prepared from orthophosphoric acid (BDH grade) and ammonium molybdate (BDH grade), except the glass labelled B/10 which was prepared from anhydrous phosphorous pentoxide and ammonium molybdate. These glasses were prepared

TABLE II Melting and annealing temperatures, density, composition, molar volume, longitudinal and shear ultrasound velocities and the elastic moduli of MoO_3–P_2O_5 glasses at room tempeature (290 K)

Glass	Melting temp. (K)	Annealing temp. (K)	Density ($g\,cm^{-3}$)	MoO_3 (mol %)	Molar volume (cm^3)	Ultrasonic velocity ($m\,sec^{-1}$)		Elastic moduli (kbar)				Poisson's ratio	Debye temp. (K)
						Long.	Shear	Long.	Shear	Bulk	Young's		
(a) *Blue Mo–P–O glasses*													
A/1	855	555	2.520	00.0	56.3	4055	2190	414	121	253	313	0.290	307
A/2	1355	575	2.629	18.2	54.1	4092	2314	440	141	252	357	0.265	318
A/3	1355	575	2.680	23.5	53.1	4120	2345	455	147	259	370	0.260	322
A/4	1395	615	2.753	29.2	51.8	4146	2407	473	159	261	396	0.246	329
A/5	1435	655	2.785	33.0	51.2	4166	2430	483	164	264	407	0.242	332
A/6	1435	655	2.840	37.5	50.2	4206	2428	502	175	269	432	0.233	338
A/7	1475	695	2.882	40.0	49.5	4240	2523	518	183	274	449	0.226	343
A/8	1475	695	2.936	44.2	48.6	4280	2568	539	194	280	473	0.219	349
A/9	1475	695	2.966	46.8	48.2	4294	2587	547	199	282	484	0.215	351
A/10	1475	695	2.968	47.2	48.1	4310	2585	551	198	287	483	0.219	354
A/11	1475	695	2.969	47.4	48.1	4315	2586	553	198	287	483	0.220	351
A/12	1475	695	2.980	48.0	47.9	4326	2609	558	203	287	493	0.214	354
A/13	1475	695	2.991	48.7	47.8	4339	2612	563	204	291	496	0.215	354
A/14	1475	695	3.004	49.7	47.6	4358	2640	572	210	292	508	0.210	358
A/15	1475	695	3.009	50.0	47.5	4375	2653	576	212	293	513	0.209	359
A/16	1475	695	3.012	50.2	47.5	4368	2641	575	210	295	509	0.211	358
A/17	1475	695	3.058	53.0	46.8	4372	2626	584	211	303	514	0.218	356
A/18	1475	695	3.072	54.0	46.6	4327	2602	575	208	298	506	0.217	353
A/19	1475	695	3.090	55.0	46.3	4288	2578	568	205	295	499	0.217	349
A/20	1475	695	3.092	55.2	46.3	4199	2525	545	197	282	479	0.217	342
A/21	1475	695	3.096	55.4	46.2	4247	2540	558	200	291	489	0.222	344
A/22	1475	695	3.100	55.6	46.1	4206	2529	548	198	284	482	0.217	342
A/23	1475	695	3.152	58.7	45.4	4174	2486	549	195	289	478	0.225	337
A/24	1475	695	3.154	58.7	45.4	4155	2482	544	194	285	478	0.223	336
A/25	1455	695	3.207	61.6	44.6	3996	2371	512	180	272	442	0.228	322
A/26	1455	695	3.214	62.2	44.5	3967	2339	506	176	271	434	0.243	317
A/27	1455	695	3.216	62.2	44.5	4068	2362	532	179	293	446	0.246	321
A/28	1435	695	3.225	62.3	44.5	3976	2348	510	178	273	439	0.232	318
A/29	1435	695	3.230	63.0	44.3	3999	2371	516	182	273	447	0.229	321
A/30	1435	695	3.234	63.0	44.3	4042	2390	528	185	281	455	0.231	324
A/31	1415	695	3.260	64.8	43.9	4007	2360	523	182	280	449	0.234	318
A/32	1415	695	3.268	65.0	43.6	4018	2367	527	183	283	452	0.234	321
A/33	1415	695	3.217	65.1	43.6	3994	2355	522	181	281	446	0.233	319
A/34	1395	695	3.282	65.8	43.6	3988	2356	522	182	283	448	0.232	319
A/35	1395	695	3.283	65.6	43.6	4004	2359	526	183	282	452	0.234	320
A/36	1395	695	3.286	65.8	43.6	3984	2350	522	181	281	447	0.234	320
A/37	1395	655	3.352	69.5	42.8	4032	2370	545	188	294	465	0.236	321
A/38	1315	655	3.362	70.0	42.6	4021	2368	544	188	293	464	0.234	321
A/39	1275	655	3.374	70.6	42.5	4013	2371	543	190	290	468	0.233	319
A/40	1255	655	3.425	73.0	41.9	3995	2357	547	190	294	468	0.233	319
A/41	1235	655	3.498	76.0	41.1	4049	2382	573	197	310	487	0.237	322
A/42	1235	635	3.501	76.7	41.0	4049	2386	574	199	309	491	0.234	322
A/43	1215	635	3.528	78.0	40.7	4053	2382	579	200	312	494	0.236	322
A/44	1215	635	3.592	80.8	40.0	4063	2388	593	205	320	507	0.236	323
A/45	1165	635	3.606	81.0	39.8	4039	2378	588	204	316	504	0.235	322
A/46	1155	635	3.695	85.2	38.9	4050	2382	606	210	326	519	0.236	322
A/47	1155	635	3.697	85.4	38.9	4055	2389	608	211	327	521	0.234	323
(b) *Green Mo–P–O glasses*													
B/1	1475	695	2.872	40.2	49.6	4558	2714	597	212	314	519	0.225	370
B/2	1475	695	2.968	46.2	48.2	4628	2786	636	230	329	559	0.216	377
B/3	1525	695	3.008	49.5	47.5	4639	2802	647	236	332	572	0.212	379
B/4	1525	695	3.009	49.8	47.5	4619	2819	650	239	331	578	0.209	382
B/5	1525	695	3.107	54.8	46.3	4730	2862	695	254	356	615	0.211	388
B/6	1525	695	3.127	55.0	45.7	4712	2843	694	253	357	614	0.223	368
B/7	1475	695	3.139	57.6	45.5	4547	2715	647	230	340	563	0.223	368
B/8	1475	695	3.280	65.2	43.7	4478	2659	658	232	349	570	0.228	360
B/9	1475	695	3.378	68.8	42.4	4420	2597	660	228	356	564	0.236	353
B/10	1425	695	3.373	69.8	42.5	4310	2535	628	217	339	537	0.235	344

in platinum crucibles (50 g capacity), using 10 ml orthophosphoric acid and varying amounts of ammonium molybdate. The solution thus obtained, was heated on a bunsen burner for about 2 h, in order to remove almost all the water content, with frequent stirring. The melt was then transferred to an electrically heated furnace at a temperature of about 1200° C for about 20 min, with frequent stirring with an alumina rod. Melts of these glasses were cast into previously heated moulds as described earlier.

The melting temperatures, annealing temperatures, and compositions (obtained by atomic absorption and

electron spin resonance (e.s.r.) spectroscopy, as described in [1]) are summarized in Table II. Glasses with the largest diameters were used to study most of the ultrasonic properties, while glasses with the smallest diameters were used to study such properties as thermal expansion, inhomogeneity, infrared absorption and atomic absorption. As the furnace enclosures were much larger than the crucibles employed temperature gradients across the melts and glasses during annealing were considered to be negligible and thus a high spatial uniformity of physical properties of the glasses was anticipated.

5. General remarks on the physical properties of Mo–P–O glasses

Glasses prepared from anhydrous MoO_3 and P_2O_5 were blue in colour and thus termed "blue" Mo–P–O glasses. The following properties were observed during the preparation of these glasses.

1. During the melting of the mixture, there was loss of oxygen, and much loss of P_2O_5 in comparison with the MoO_3. The loss of P_2O_5 increases as the amount of MoO_3 in the starting mixture decreases. Hence, it is impossible to calculate even approximately, the correct composition of these glasses from the composition of the starting materials. Thus, chemical (or other equivalent methods) analysis of these glasses was required for our structural investigation.

2. In the system Mo–P–O, the limits for the glass formation i.e. the range in which glass can be prepared is $0 < MoO_3\,\text{mol}\,\% < 86$.

3. The viscosity of the melt increases with the amount of MoO_3.

4. The melting temperature, i.e. the temperature at which the melt can be stirred, increases with the amount of MoO_3 and reaches a maximum value of about 50 mol % MoO_3. After further addition of MoO_3 content, the melting temperature decreases.

5. Glasses below 29 mol % MoO_3 were much more hygroscopic than the rest of the series. All glasses were stored under silica gel in an evacuated desiccator.

6. Glasses with a low content of MoO_3 were light blue in colour. The colour intensity increases with the amount of MoO_3 and eventually becames opaque.

The following properties were observed during the preparation of more reduced Mo–P–O from the mixture of orthophosphoric acid and ammonium molybdate.

1. When the ammonium molybdate was mixed with orthophosphoric acid, the solution became warm, and when heated over a bunsen burner, the colour of the solution changed to yellow and then finally to dark green. Therefore, these glasses were termed "green" Mo–P–O glasses. Moreover, the viscosity also increased with the heating of the solution.

2. These green Mo–P–O glasses were more stable against atmospheric water attack, and also the solubility in hot water was very low, when compared with blue Mo–P–O glasses having nearly the same composition as the green Mo–P–O glasses.

3. During stirring of the solution, the melt gathered on the tip of an alumina rod, changed its colour from green to blue, when examined after dipping the tip in water. When the same tip was dehydrated on a flame, the colour of the melt changed back to its original colour.

4. The melting tempeature and viscosity was high compared with corresponding blue Mo–P–O glass of same composition.

6. Density measurement and results

The densities were measured by the Archimedes method, using toluene (density = 0.864 to 0.867 $g\,cm^{-3}$ at 20° C) as an immersion liquid. The density of each glass was then obtained using the relation

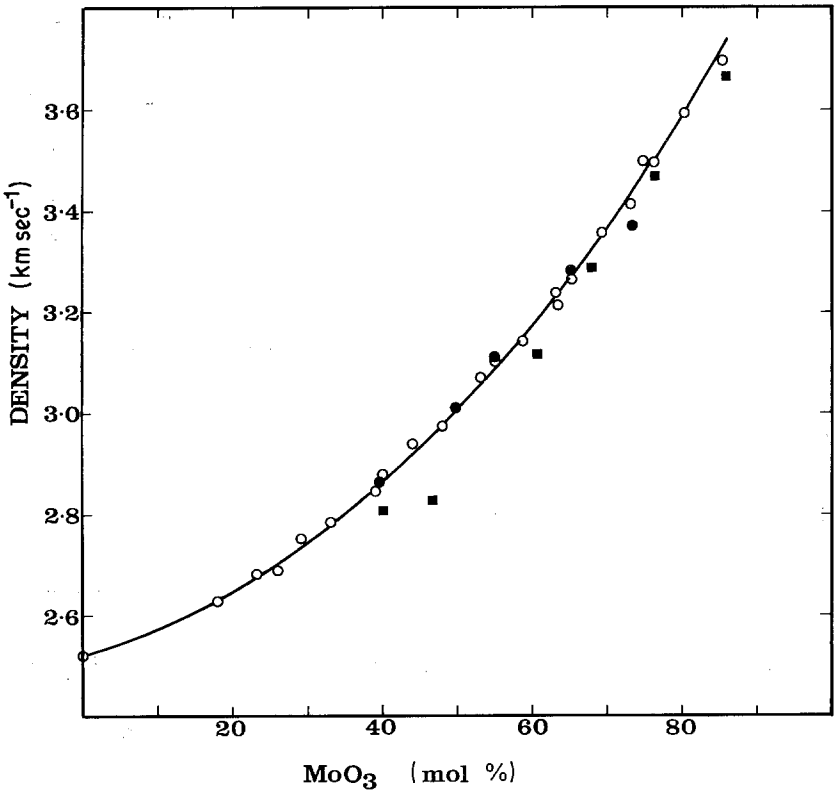

Figure 3 Variation of density with composition (mol %) for the vitreous system MoO_3–P_2O_5. The chemical composition of these glasses (denoted by full and open circles) was obtained by an atomic absorption measurement of molybdenum content only. (●) MoO_3–P_2O_5 (green glasses), (○) MoO_3–P_2O_5 (blue glasses), (■) data from [4].

TABLE III Effect of melt temperatures on glass composition for Mo–P–O glasses

Glass no.	Melt temp. (K)	Melting time (min)	Annealing temp. (K)	Annealing time (min)	Density ($g\,cm^{-3}$)	MoO_3 (mol %)	P_2O_5 (mol %)
C/33	1395	30	695	120	3.27	65.0	35.0
	1475	30	695	120	3.32	67.2	32.8
	1535	30	695	120	3.36	70.0	30.0

$$\varrho = \frac{\varrho_0(M - M_t)}{M - M_t - (M^1 - M_t^1)} \quad (1)$$

where ϱ_0 is the density of toluene, M and M^1 are the weights of the glass when suspended by a thread in air and toluene, respectively, the M_t and M_t^1 are the weights of the thread in air and toluene, respectively. The results are absolutely accurate to 0.05%, and relatively accurate to the number of significant figures quoted in Table II, i.e. repeated density measurements agreed within $\pm 0.01\%$. Results obtained are also plotted in Fig. 3.

The density increased smoothly with increasing amount of MoO_3, (determined from the atomic absorption as described in [1]). The densities found in this series closely resemble those found in the same series prepared by Kierkegaard [4], who determined the composition of glasses by chemical analysis. However, significant differences are found in the density of Mo–P–O glasses of reportedly the same composition, in cases where the authors [12–14] had defined their compositions as the composition of the mixture prior to melting.

Since glass history, i.e. preparation technique, melting temperature, annealing tempeature and time, melting atmosphere, cooling rate, etc., has some effect on glass properties such as density, composition, etc., the following arguments, perhaps, could resolve the discrepancies in the values of certain physical quantities attributed to a given glass by different authors.

1. If the melt tempeature employed is much higher than the "correct" melting tempeature, then there will be a much greater loss of phosphorous pentoxide relative to molybdenum trioxide (see Table III). And so the density of glass will increase with increasing temperature of the melt.

2. If a longer melting time is employed, then the composition will also change, i.e. the amount of MoO_3 will increase with the time to a certain extent. Again this will cause the density to increase (see Table II).

These considerations make it clear that the chemical analysis (or equivalent methods) of all glasses prepared in open crucibles is essential for any quantitative discussion of the compositional dependence of properties. Any data in the literature presented without such analysis having been made, must be treated with particular care when comparisons are attempted.

7. Molar volume

In binary phosphate glasses. from the curves of molar volume, refractive index and density versus composition, Kordes [15] has divided these glasses into normal and anomalous glasses (see Section 5.1.1). In normal glasses the curves are smooth, while in anomalous glasses, the curves show a distinct discontinuity at a composition corresponding to 50 mol % MoO_3.

In our binary molybdenum–phosphate glasses, the

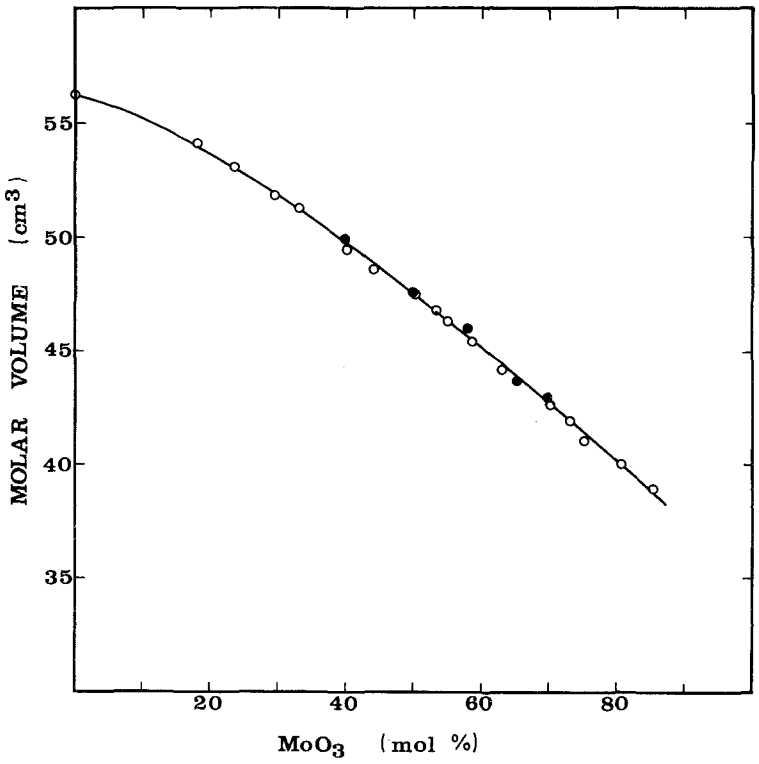

Figure 4 Effect of composition on molar volume (i.e. the volume containing x mol MoO_3 and $(1 - x)$ mol P_2O_5 in the system MoO_3–P_2O_5. (●) Green glasses, (○) blue glasses.

density and molar volumes show smooth variations Figs. 3 and 4) with composition, without any discontinuities in the curves. Thus, one can regard these Mo–P–O glasses as normal glasses in the above sense, although in our Mo–P–O glasses there is no evidence of molybdenum entering the holes of the network or producing single-bonded oxygens, which is what ought to happen according to the Kordes and Tarasov model of "normal glasses". On the contrary, MoO_3 acts as a network-former rather than network-modifier throughout the complete Mo–P–O range, by increasing the crosslink density of P_2O_5. These findings are based on our elastic properties, and infrared absorption data, to be published separately.

8. Ultrasonic measurements

All the Mo–P–O glasses were lapped initially with 600 grade silicon carbide powder on a lapping machine (Flexibox model 12 A), to obtain two approximately parallel faces. For this purpose a sample jig consisting of a mould having almost the same cross-sectional dimensions as the casting mould but with an adjustable depth, was employed [16]. Those glasses needing to be cut, were cut to the required size on a diamond cutting instrument.

It is essential to obtain glass specimens with two optically flat and parallel faces, for accurate velocity measurements. This was achieved by the use of a precision polishing machine (Multipol 2), with the aid of a special jig (MR, Mk 2) holding the specimen, and an autocollimator, all of which were supplied by Metals Research Ltd. In their final form glass specimens were about 1.6 cm diameter and 3.5 to 5 mm thick.

Ultrasonic wave compressional and shear wave velocities were measured using the pulse-echo technique. Transit times between the first cycle of successive echoes were measured to 0.04% absolute and 0.5 nsec relative accuracy. The time measurement system consisted of a digital delay generator (Berkeley Nucleonics model 7030) which gave a potential precision for relative measurements of ± 200 psec, this figure being twice the time jitter of the delay pulse relative to the trigger pulse. The attenuation in the Mo–P–O glasses was typically 1 dB μsec^{-1}. The specimens were previously coated with aluminium by a vacuum evaporation technique, annealed at 200° C and subsequently stored under silica gel in an evacuated desiccator for at least a week in order to achieve a firm aluminium coating.

For each glass, correct cyclic matching between echoes was achieved by first using broad band instrumentation which permitted the first $\frac{1}{4}$ cycle of r.f. above noise, in consecutive echoes, to be readily observed. Then narrow band instrumentation (Arenberg) was next employed and the approximate transit times obtained by the broad band technique were used to enable corresponding pairs in successive echoes of the narrow band presentation, to be selected.

X-cut quartz transducers of 1 cm diameter, and 15 MHz fundamental frequency were employed to generate longitudinal waves. Shear waves were generated using 10 and 15 MHz AT-cut quartz crystals of 1 cm diameter. Nonaq stopcock grease and shear wave paste (Krautkrämer ZYG) were used as a complant between the transducer and the specimen for the longitudinal and shear waves, respectively. All transducers were uncoated, the aluminium coating on the glass specimens providing the necessary earth electrode for the transducers, and a brass sprung contact button acting as the other electrode. A special sample holder was designed to allow the contact pressure on the crystal bond specimen to be adjusted until the necessary exponentially decaying echo patterns were obtained.

The values of elastic moduli and Poisson's ratio were calculated using the standard relationships $\varrho V_L^2 = L$, $\varrho V_S^2 = G$, $L = K + 4/3G$, $G = E/2(1 + \sigma)$, $\sigma = E/2G - 1$, where L, G, K, and E, are the longitudinal, shear, bulk, and Young's modulus, respectively, and σ is Poisson's ratio. In case they should be subsequently useful for comparison with infrared and conductivity data, the Debye temperature of each glass was obtained using the following expression:

$$\theta_D = \frac{h}{k}\left[\frac{3\varrho N_a P}{4\pi M}\right]^{1/3} V_m \qquad (2)$$

where V_m is the mean sound velocity, given by the following equation:

$$V_m = \left[\frac{1/V_L^3 + 2/V_S^3}{3}\right]^{-1/3} \qquad (3)$$

and P is the number of atoms per unit formula, N_a is Avogadro's number, ϱ is the density, M is the molecular weight, h is Planck's constant and k is Boltzmann's constant.

The ultrasonic wave velocities, elastic moduli, Poisson's ratio and Debye temperatures for the Mo–P–O system are given in Table II and the compositional dependence of these quantities are plotted in Figs. 5 to 11.

9. Elastic moduli of blue glasses: results and interpretation

The most obvious features of the results are the discontinuities in the compositional gradients of the elastic moduli at compositions (i.e. mol % MoO_3) approximating to the compositions of molybdenum metaphosphate and pyrophosphate crystals. In the following discussion, we attempt qualitative interpretation of how the elastic moduli and Poisson's ratio vary with the glass composition. For this we shall need to make some intelligent guesses as to the coordinations of the molybdenum and phosphorus atoms in the glasses. For this purpose, following the discussions of Section 3 we shall assume that the glass consists of mixtures of the structural groupings that occur in the crystalline phases of the Mo–P–O system (Fig. 2). If the glasses are represented by the general chemical formula:

$$x\,Mo_2O_5\; y\,MoO_3(1 - x - y)P_2O_5$$

where x and y are mole fractions, all Mo^{5+} cations are represented by Mo_2O_5, and M^{6+} cations represented

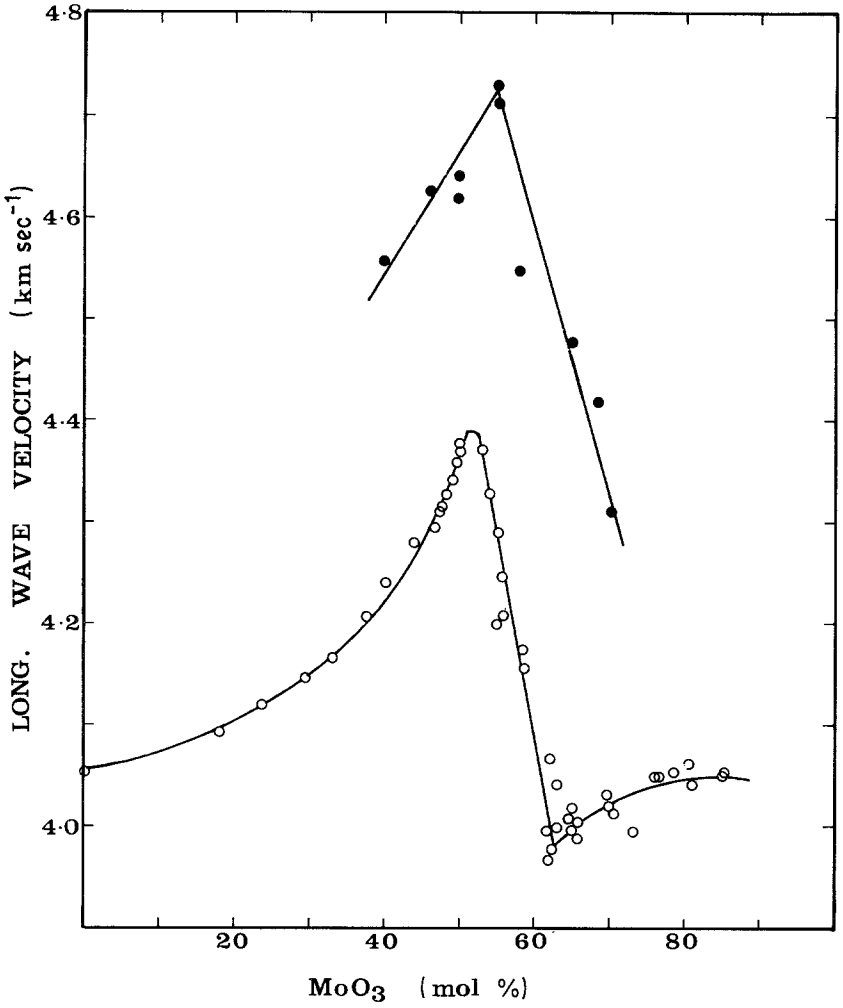

Figure 5 Dependence of the velocity of longitudinal sound waves on composition. MoO_3–P_2O_5 (●) green glasses, (○) blue glasses.

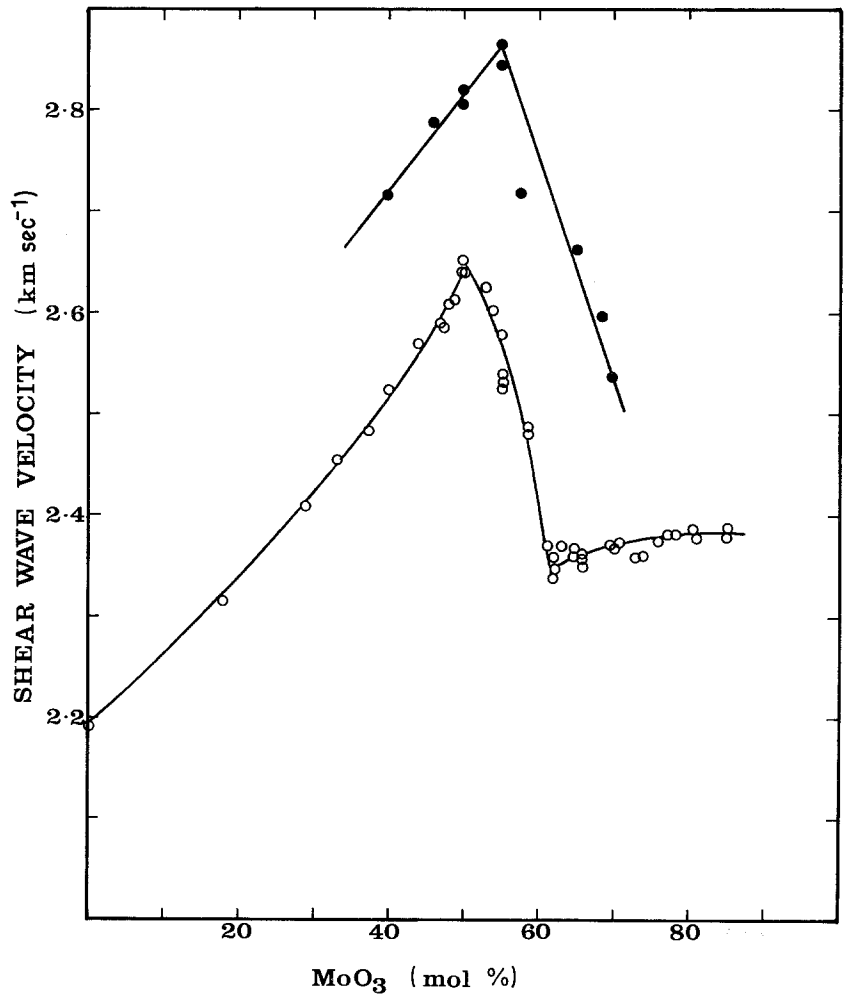

Figure 6 Dependence of the velocity of shear waves on composition. MoO_3–P_2O_5 (●) green glasses, (○) blue glasses.

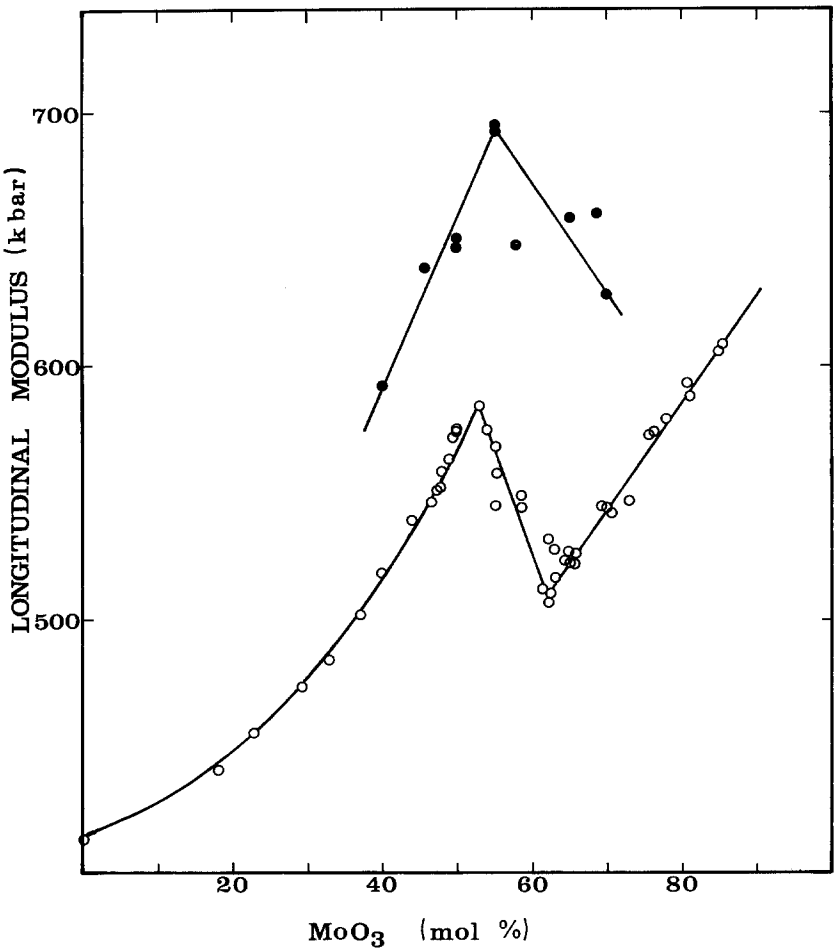

Figure 7 Compositional dependence of longitudinal modulus. MoO_3–P_2O_5 (●) green glasses, (○) blue glasses.

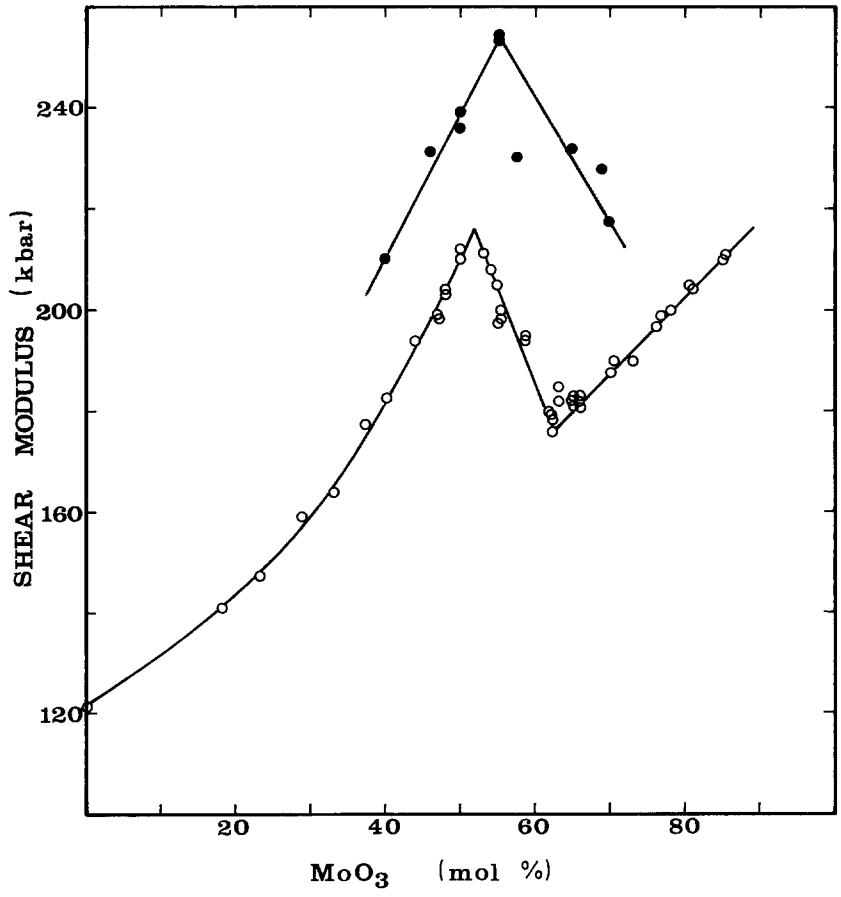

Figure 8 Variation of the shear modulus with composition. MoO_3–P_2O_5 (●) green glasses (○) blue glasses.

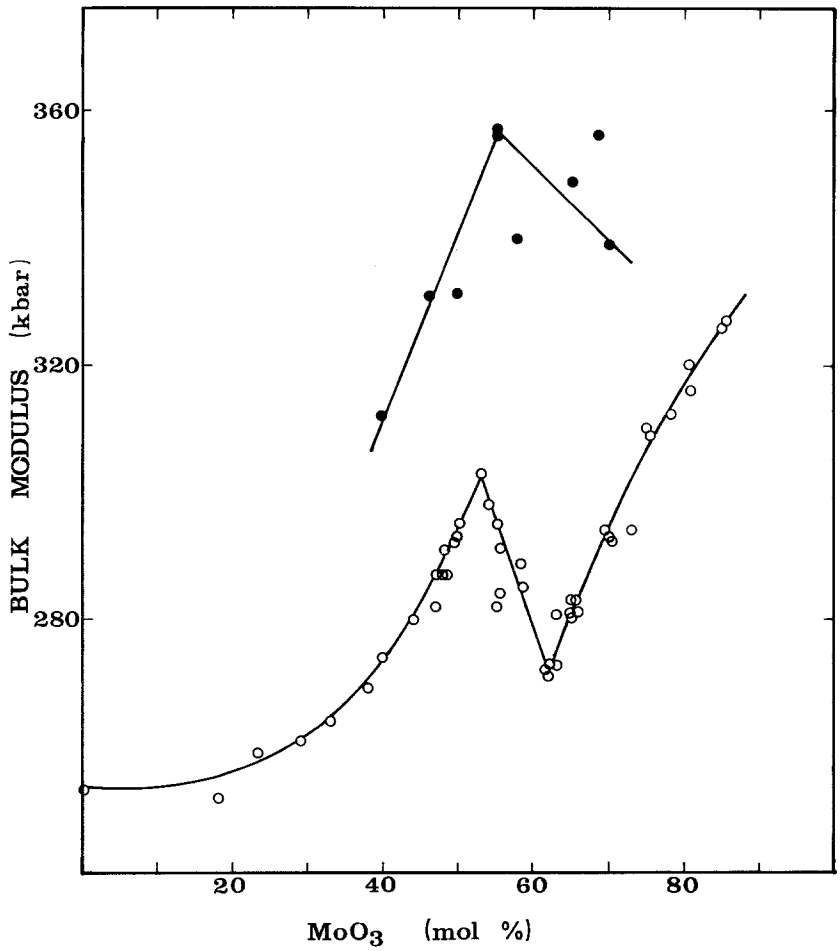

Figure 9 Dependence of the bulk modulus on the composition. MoO_3–P_2O_5 (●) green glasses; (○) blue glasses.

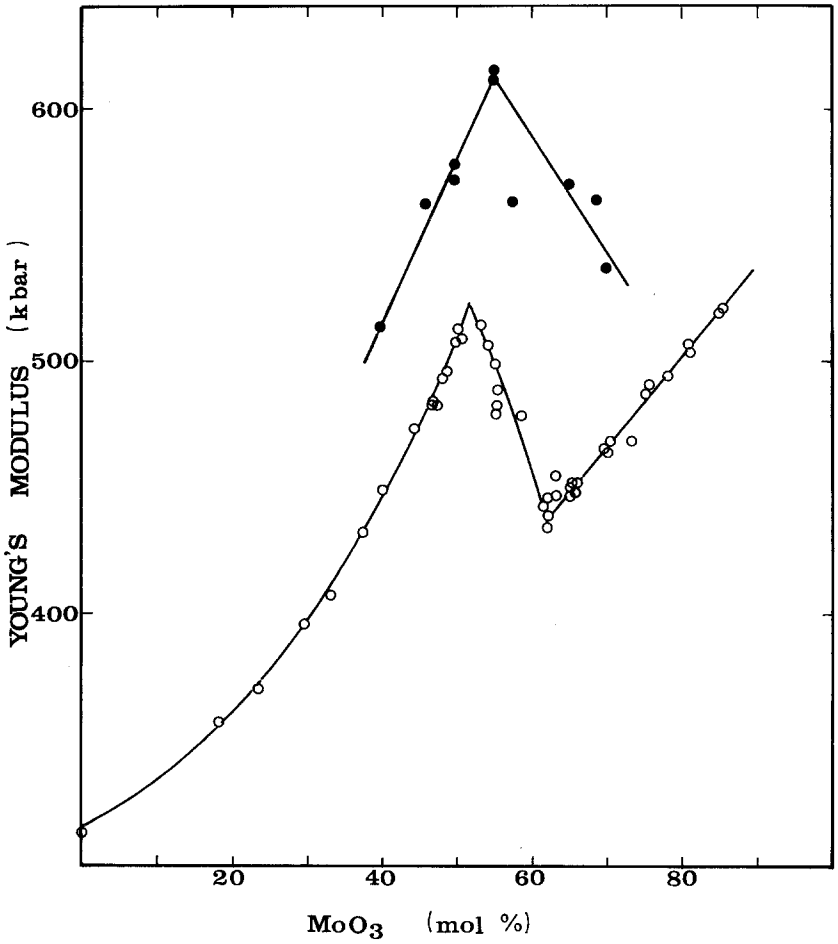

Figure 10 Compositional dependence of Young's modulus. MoO_3–P_2O_5 (●) green glasses, (○) blue glasses.

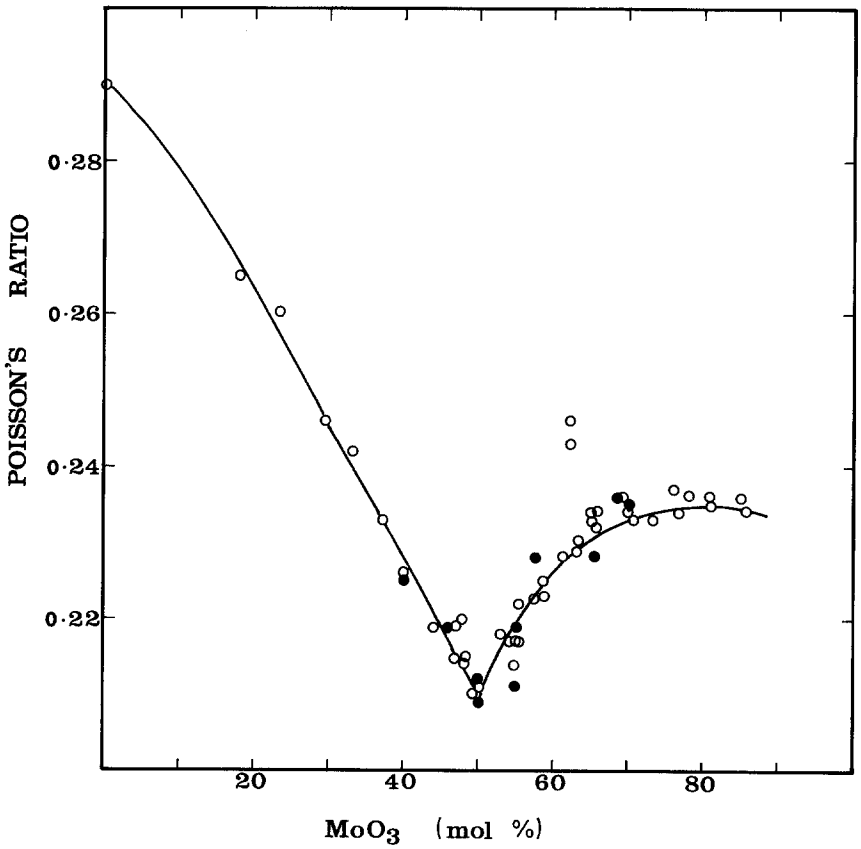

Figure 11 Variation of Poisson's ratio with composition. MoO_3–P_2O_5 (●) green glasses (○) blue glasses.

by MoO_3; the corresponding mole fractions of the structural groupings, assuming that all the M^{5+} cations are contained in the form of $MoOPO_4$, are given by

$$\left[\frac{y}{1-y}\right] MoO_2(PO_3)_2 \left[\frac{2x}{1-y}\right] MoOPO_4 \cdot \left[\frac{1-2x-2y}{1-y}\right] P_2O_5, \quad 0 < MoO_3 < 50\,\text{mol}\,\%$$

$$\left[\frac{2-4x-3y}{1-y}\right] MoO_2(PO_3)_2 \cdot \left[\frac{2x-2y-1}{1-y}\right](MoO_2)P_2O_7 \cdot \left[\frac{2x}{1-y}\right] MoOPO_4,$$

$$50 < MoO_3 < 65\,\text{mol}\,\%$$

$$\left[\frac{1-2x-y}{4x+2y-1}\right](MoO_2)_2P_2O_7 \cdot \left[\frac{2x}{4x+2y-1}\right] MoOPO_4 \cdot \left[\frac{3y+4x-2}{4x+2y-1}\right] MoO_3,$$

$$65 < MoO_3 < 85\,\text{mol}\,\%$$

The compositional dependence of x and y in the chemical formula, deduced from the chemical analysis data of Patel and Bridge [1] is plotted in Fig. 12a. The corresponding mole fractions of the structural groupings proposed to be present, are plotted in Fig. 12b. It will be observed that sharp peaks in metaphosphate and pyrophosphate groups occur at about 50 and 66 mol % Mo_2O_5 + MoO_3 content, whilst a broad, rather flat peak is orthophosphate content stretching from about 50 to 62 mol % total oxide content, is obtained. In all tables and figures other than Fig. 12, the MoO_3 contents presented have been compiled (from the chemical analysis data of [1]) on the assumption that all the molybdenum content is in the MoO_3 form. This has been done to simplify the discussion and presentation. The MoO_3 content calculated in this way is at the most 1 mol % higher than the true Mo_2O_5 + MoO_3 content and 2 mol % higher than the true MoO_3 content. Such small differences have no significance in the present qualitative discussions.

Given this information, two qualitative interpretations of the experimental elastic behaviour are possible, based on models developed for pure oxide glasses by Bridge *et al.* [17]. We present them both because they highlight different structural features.

9.1. Ring deformation model of bulk modulus

According to this model, the bulk modulus of a

TABLE IV Effect of melt temperature on glass composition for Mo–P–O glasses

Glass no.	Melt temp. (K)	Melting time (min)	Annealing temp. (K)	Annealing time (min)	Density ($g\,cm^{-3}$)	MoO_3 (mol %)	P_2O_5 (mol %)
D/38	1275	30	645	120	3.36	70.0	30.0
	1275	60	645	120	3.39	72.2	27.8
	1275	100	645	120	3.46	74.8	25.2

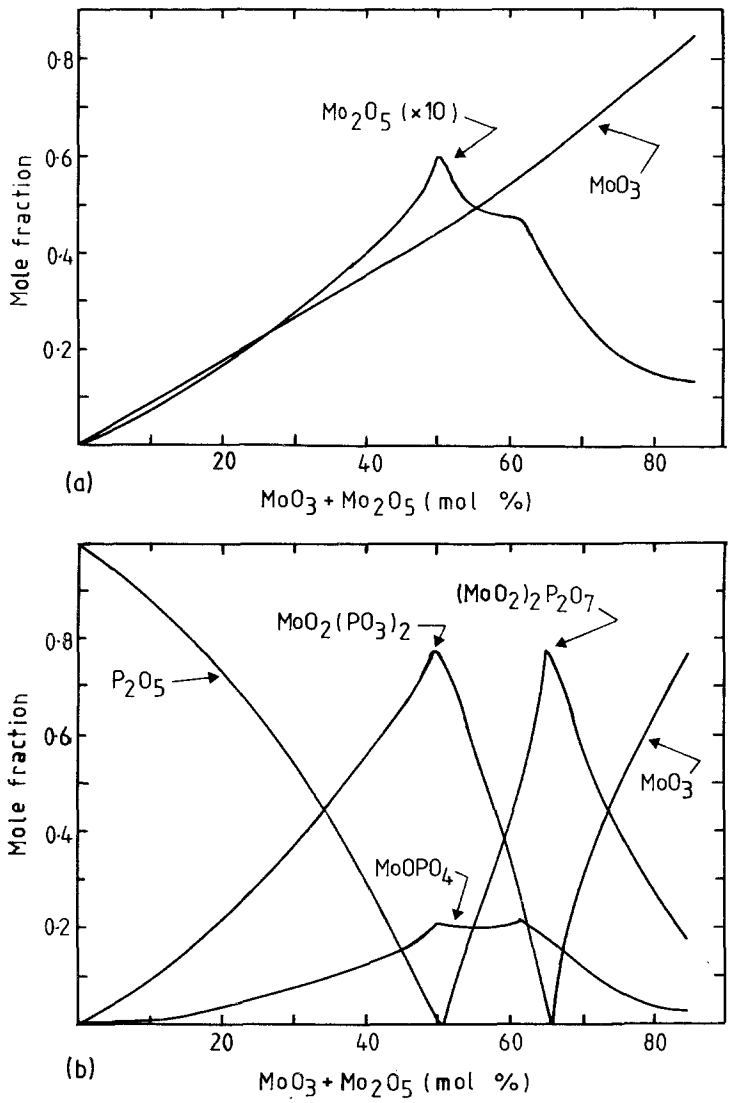

Figure 12 (a) Chemical composition of the blue Mo–P–O glass system expressed in the form $xM_2O_5yMoO_3(1 - x - y)P_2O_5$, where x and y are mole fractions. (b) Composition of the same glass system expressed as mole fractions of MoO_3, $MoO_2(PO_3)_2$, $(MoO_2)_2P_2O_7$, $MoOPO_4$, and P_2O_5.

structure consisting of a three-dimensional network of A–O bonds (A = cation, O = oxygen atom) can be expressed in the form:

$$K = \text{constant}\,\frac{F_b}{(l)^n} \tag{4}$$

where F_b is the A–O bond bending force constant which to a first approximation may be taken as proportional to the bond stretching force constant F; and l is the diameter of the atomic rings, i.e. the smallest closed circuit of A–O network bonds; the rings being assumed to take the form of planar circles, for simplicity, so that $l = (N_b r)/\pi$ where N_b is the number of A–O bonds in the ring and r is the A–O bond length. The constant is determined empirically and so is the power n, which is typically high – say 4. The model was originally proposed to account for the bulk moduli of the pure vitreous oxides whose ring sizes were assumed to be similar to the ring sizes occurring in the analogous crystal structures and which were known from X-ray crystallography. The model is readily adapted, in principle, to mixed oxide glasses by performing an average procedure for F over all the different types of network bond and ring size. However, in practice, one can see many difficulties relating to (i) deciding what kinds of rings are present which require assumptions of the type made in plotting, Fig. 12; (ii) the problem of how to average when a number of contrasting ring sizes are present. Only a qualitative discussion seems worthwhile at this stage. For this purpose we shall assume that for structures in which the groups share corners only, when a glass composition changes gradually, reductions in average crosslink density per cation lead to increases in average ring size, and vice versa – but with some important exceptions that will subsequently become apparent. By examination of Fig. 13 and the crystal structures in Figs. 2a to e, we can decide on how crosslink densities vary (qualitatively) with glass composition. We can also perform an independent check on how average ring size varies with composition by a direct inspection of the ring sizes of the structural groups, displayed in Fig. 2.

Bridge *et al.* also argued that the chief determinant of the level of Poisson's ratio in the pure inorganic oxide glasses is crosslink density, the former decreasing as the latter increases. If this argument were extended to multicomponent glasses we could assume empirically that

$$\sigma = g(\bar{n}_c) \tag{5}$$

where $\bar{n}_c$ is the mean crosslink density per cation and g is a function which decreases slowly as $\bar{n}_c$ increases. If bulk modulus and Poisson's ratio can be understood from Equations 1 and 2 it follows that the

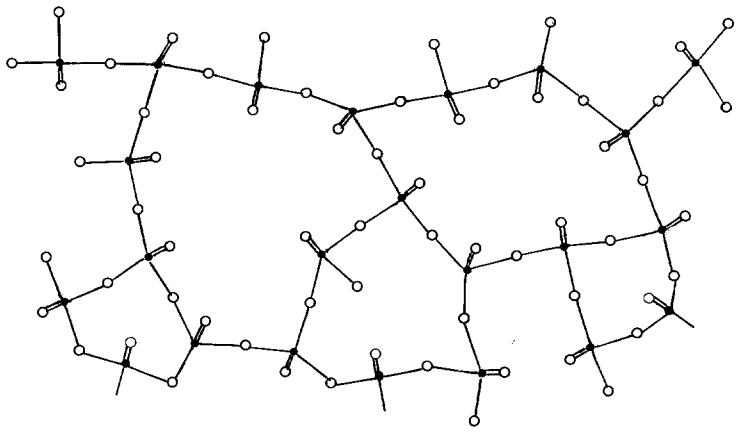

Figure 13 A schematic two-dimensional illustration of vitreous P_2O_5. The average crosslink density per cation is one and Poisson's ratio is 0.29 (experimental value), and the average ring size is 12.5 anions + cations. ●, phosphorus atoms; ○, oxygen atoms.

behaviour of the remaining elastic moduli are also accounted for.

In the absence of any better information we assume that for all bond types, the bending force constants are proportional to the stretching force constants. The lengths of the various kinds of M–O bond in the crystal structures shown in Fig. 2, are ~0.2 nm, whilst the various types of P–O bond are ~0.16 nm long. From the force constant–bond length relationship for oxide glasses shown in Fig. 1 of Bridge *et al.* [17], it follows that the Mo–O stretching force constants are less than one half the P–O force constants. Thus, with increasing Mo content in Mo–P–O glasses, it is clear that $\bar{f}_b$ must decrease continuously. However, the bulk moduli of all Mo–P–O glasses exceed that of pure P_2O_5 glass, and generally increase with molybdenum content. On the ring deformation model we conclude that the "ring size effect" dominates the observed levels of bulk modulus. Now since the Mo–O bond lengths are substantially longer than the P–O bonds, ring sizes would increase with molybdenum content if the number of cations + anions in a ring remained constant. So we can only explain the observed increases in bulk modulus in terms of a reduction in the number of cations + anions in the rings.

Fig. 13 shows the proposed structure of pure P_2O_5 glass. The average ring size (cations + anions) is 12.5, approximating to the value suggested by Bridge *et al.* [17]. The addition of MoO_6 octahedra to this network will transform some of the P=O bonds into crosslinking (bridging) bonds of the type Mo–P–O and P–O–P. The progressive rupture of P=O bonds with increasing molybdenum content is convincingly demonstrated in the infrared spectra of our glass series (to be published separately). To this effect we must add the increased crosslink density of the molybdenum atom which depending on the type of environment proposed in Figs. 2a to e, varies between 2 and 4, compared with the value of 1 for phosphorus in P_2O_5. Now by inspection of Fig. 12 we find that the mean crosslink density per cation must increase gradually from 1, to somewhere between 2 and 4 at 50 mol % MoO_3 content, and there will be a commensurate decrease in Poisson's ratio according to Equation 5. This also suggests that the ring size in anions + cations should decrease progressively in this composition range. Comparing Figs. 2 and 12 we can confirm this directly as a gradual replacement of P_6O_6 and MoP_2O_3 (metaphosphate) and $Mo_2P_2O_4$ (orthophosphate) rings. Figs. 14 and 15 show schematically the proposed ring structures for 26 and 50 mol % MoO_3 glass, respectively. As drawn, the average ring sizes are 9.8 and 6.9 cations + anions, respectively. The large increase in bulk modulus in the range $0 < MoO_3 < 50$ mol % is now readily understood. In general terms the structures drawn in Figs. 15 and 16 can be described as assemblies of MoO_6 octahedra and single PO_4 tetrahedral groups or PO_4 chains of varying length consistent with Keirkegaard's chromotographic observations, with corner sharing only in accordance with Zachareisen's model of glass.

As the MoO_3 content is increased from 53 to 66 mol % our model of structural groupings (Fig. 12) suggests that the metaphosphate and orthophosphate groups start to be replaced by pyrophosphate groups.

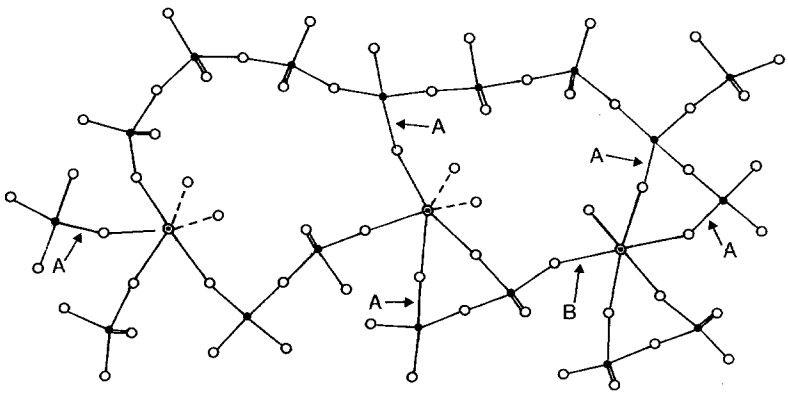

Figure 14 A schematic two-dimensional illustration of the proposed structure of Mo–P–O glass having 26 mol % MoO_3. Arrow A shows the formation of Mo–O–P and P–O–P bonds from P=O bonds. Arrow B shows an MoO_6 octahedron in an "orthophosphate" configuration, i.e. there are two additional bridging bonds formed by the reduction of a molybdenum ion. The remaining octahedra are in a metaphosphate configuration, i.e. two dangling bonds. Note the presence of some MoP_2O_3 rings typical of metaphosphate grouping. The average ring size is 9.8 cations + anions and the average crosslink density per cation is about 1.5. ●, phosphorus atoms; ○, oxygen atoms; ⊙, molybdenum atoms.

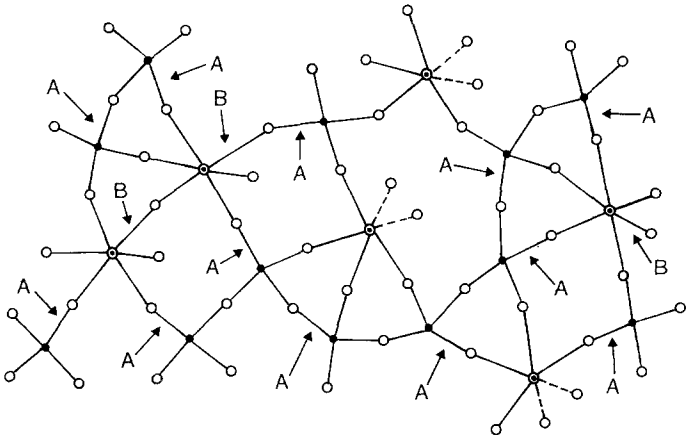

Figure 15 A schematic two-dimensional illustration of the proposed structure for Mo–P–O glass having 50 mol % MoO_3. Arrow B shows the effect of the reduction of the molybdenum atom and arrow A shows the formation of bridging bonds from P = O bonds. Note the preponderance of MoP_2O_3 (metaphosphate) and $Mo_2P_2O_4$ (orthophosphate) rings. The average ring size is 6.9 cations + anions and the average crosslink density per cation is ~2.5. ●, phosphorus atoms; ○, oxygen atoms, (⊙), molybdenum atoms.

The crosslink density per cation of the latter lies halfway between that of the two former groups which are 2 and 3, respectively. So on balance little change in crosslink density per cation is anticipated in this composition range. This is reasonably consistent with the behaviour of Poisson's ratio, which starts to increase from its minimum value at 53 mol % MoO_3 content, but only slightly. In contrast the bulk modulus falls much more sharply suggesting a dramatic increase in ring size. This is due to the replacement of the mixture of MoP_2O_3 (metaphosphate) and $Mo_2P_2O_4$ (orthophosphate) rings (i.e. 6 cations + anions < mean ring size < 8 cations < anions) by $Mo_2P_2O_4$ (pyrophosphate) rings (i.e. 8 cations + anions). We can arrive at the same conclusion without appeal to the detailed structures of Fig. 2, as follows: in the 50 mol % MoO_3 glass as drawn in Fig. 15, there is a high occurrence of MoO_3 tetrahedra separated by only a single PO_4 group, tending to produce small rings of cations + anions because the average crosslink density for MoO_6 groups (averaged over M^{5+} and M^{6+} ions) is greater than that occurring in PO_4 chains. In the glasses of higher molybdenum content, the substitution of P_2O_7 groups for single PO_4 groups pushes the MoO_6 octahedra further apart thus increasing average ring sizes. In Fig. 16, the proposed structure for 66 mol % MoO_3 glass, the average ring size is 9 cations + anions.

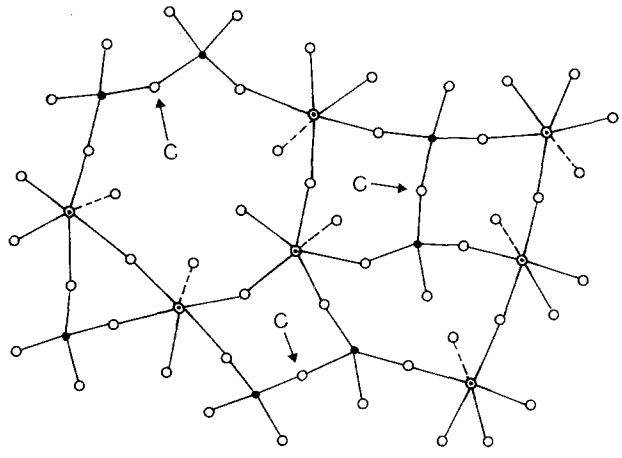

Figure 16 A schematic two-dimensional illustration of the proposed model for Mo–P–O glass having 66 mol % MoO_3. Arrow C shows the P_2O_7 groups connecting the MoO_6 octahedra. The average crosslink density is 2.5. Note the preponderance of $Mo_2P_2O_4$ (pyrophosphate) rings. Most of the MoO_6 octahedra are in a "pyrophosphate" configuration with a single dangling bond and the average ring size is 9 cations + anions. ●, phosphorus atoms; ○, oxygen atoms; ⊙, molybdenum atoms.

Finally we come to the 66 to 83 mol % MoO_3 composition range. Inspection of Fig. 12 shows that octahedral groups as in pure MoO_3 crystal gradually replace pyrophosphate groupings. From Figs. 2c and e the mean crosslink density per cation can only increase to a limited extent, in the range 2.5 to 3, in agreement with the very slow increase in experimental Poisson's ratio in this composition range. However, inspection of the same figures show that large $Mo_2P_2O_4$ pyrophosphate rings (8 cations + anions) become gradually replaced by very small MoO_2 rings (i.e. 4 cations + anions). The steep rise in bulk modulus in this composition range is thus readily understood. In Fig. 17 the proposed structure of 80 mol % MoO_3 glass has an average ring size of 6.4 anions + cations, a substantial number of pyrophosphate groups still being present. It will be noted that the suggested structure involves some edge sharing of MoO_6 octahedra (i.e. sharing of some oxygens with three molybdenum cations) as in the MoO_3 model. Although this is in contradiction with Zachareisen's model of glass, it is the only obvious explanation of the steep rise in bulk modulus for MoO_3 contents, and moreover the idea is substantiated by infrared data (to be published separately).

9.2. Bond compression model

In Bridge *et al.* [17] it was shown that for three-dimensional network structures containing only one type of bond, the bulk modulus calculated on the assumption that isotropic compression of the structure results in uniform reductions in bond lengths without any change in bond angles, is given by

$$K_{bc} = n_b r^2 f/9 \quad (6)$$

where n_b is the number of network bonds per unit volume, r is the bond length, and f is the first order stretching force constant, and higher order force constants and bond–bond interactions are neglected. One can easily extend this formula to multi-component oxide glasses by writing

$$K_{bc} = \sum_i \frac{n_i r_i^2 f}{9} \quad (7)$$

where the sum is taken over all the types of network

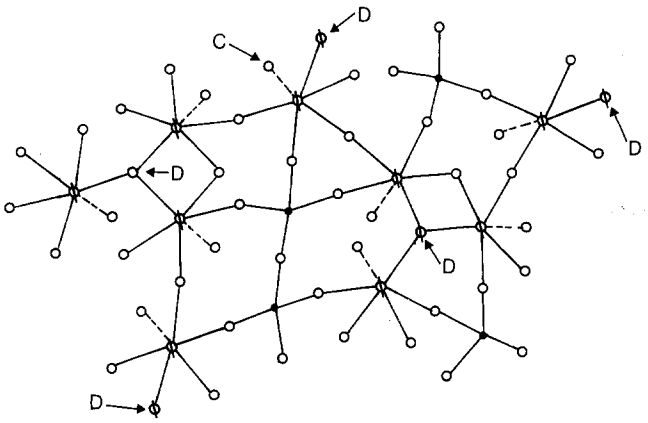

Figure 17 A schematic two-dimensional illustration of the proposed structure of Mo–P–O glass having 80 mol % MoO_3. Arrow D shows the edge sharing of MoO_6 octahedra. The remaining octahedra (for e.g. arrow C) are in the pyrophosphate configuration with a single dangling bond. The average ring size is 6.4 anions + cations and the average crosslink density per cation is about 2.4. The structure consists predominantly of a mixture of small Mo_2O_2 (molybdenum trioxide) rings and relatively large (pyrophosphate) $Mo_2P_2O_4$ rings. ●, phosphorus atoms; ○, oxygen atoms; ⊙, molybdenum atoms, ⊖ represents oxygen atom sharing three molybdenum atoms.

bonds labelled 1, 2, . . . , i, . . . , in the structure. Usually Equation 6 will be found to overestimate the experimental modulus K_e by a factor of 3 to 10. The ratio K_{bc}/K_e forms a rough measure of the extent to which bond bending processes are involved in isotropic deformation and it has been argued further that, at least for the pure inorganic oxide glasses, K_{bc}/K_e will increase systematically with ring size, provided the ratio of bond bending to stretching force constants for the different glasses is the same. So empirically we can write

$$K_e \simeq K_{bc} F(\bar{l}) \tag{8}$$

where F is a function which decreases as the average ring sizes $\bar{l}$ (where for any one ring $l = \Sigma_i$ number of bonds × bond length of bond type i/π) increases, and takes a maximum value of ~ 1 for a structure of small rings like diamond. Now as the molybdenum content of Mo–P–O glasses is gradually increased since f decreases as $\sim r^{-3}$ (Fig. 1 of [17]), $r_i^2 f_i$ is expected to decrease as $\sim \bar{r}_i$, i.e. by about 25% over the entire vitreous compositional range. The number of network bonds per molybdenum atom is never less than 4 whilst for the phosphorus atom, it never exceeds 2 (when the P=O bond is ruptured). Moreover the molar volume of Mo–P–O glasses (Fig. 4) decreases by 30% over the glass composition range. We conclude that $\bar{n}_i$ increases much more rapidly than 25% over this range. So K_{bc} evidently increases progressively with MoO_3 content. Apparently then there is no need to postulate any dramatic change in ring size except for the composition region 50 to 66 mol % MoO_3 – the only instance where the K_e variations contradicts the trend of K_{bc} by decreasing very sharply. In this case we reach the same conclusion as on the ring deformation model, i.e. a pronounced structural rearrangement leading to substantial increases in ring size occurs in this composition regime, and it consists of the replacement of alternate sequences of MoO_6 octahedra and PO_4 tetrahedra, by P_2O_7 groups separating the MoO_6 groups. Also assisting in the reduction of the bulk modulus in this region is the steep negative compositional gradient of the Mo^{6+}/Mo^{5+} ratio, i.e. the 4 network bonds per Mo^{6+} ion are replaced by the fewer network bonds per Mo^{5+} ion. This reduction effect probably introduces an inflexion or plateau region in the curve of K_{bc}/K_e against composition.

10. Results and discussion: green glasses

A complete range of green Mo–P–O glasses has not been studied, but enough results were obtained to discern the trend of their physical properties, including the elastic moduli. Although density, and molar volume of the two glass series are similar:

1. Green glasses show about a 14% increase in all elastic modulii for any given composition with blue Mo–P–O glasses;

2. The green glasses are more reduced, i.e. there are a greater number of Mo^{5+} ions present (Table I and [1]). Assuming as before (Fig. 12) an orthophosphate environment for the Mo^{5+} ions, this implies a greater proportion of molybdenum atoms with crosslink densities of 4 rather than 3 or 2 with corresponding decreases in Poisson's ratio (by Equation 5). On our assumption that atomic ring sizes decrease with increasing crosslink densities, then the 14% increase in moduli values in reduced glasses are readily understood, on our ring deformation model. Also, on the understanding that increased crosslink density leads to increased numbers of network bonds per unit volume, the same conclusion would be reached on the bond compression model. However, if one envisages the reduction process as one of converting MoP_2O_3 (metaphosphate) rings into $Mo_2P_2O_4$ (orthophosphate) rings, a contrary conclusion that the moduli should decrease, would be obtained, on the ring deformation model. This anomaly cannot be resolved in terms of the present qualitative approach. A tentative suggestion is that the bending force constants for the Mo^{6+} ions are much higher (i.e. perhaps by a factor of 2 or more) than for the Mo^{5+} ions, thus invalidating our initial premise of constant ratios of bending to stretching force constants.

11. Annealing effect on Mo–P–O glasses

Some investigators [14, 18, 19] have studied the effect of annealing temperatures on the electrical properties of binary phosphate glasses. The annealing effect on $CuO–P_2O_5$ glasses showed that by increasing the annealing temperature, both the activation energy and conductivity decreased [18]. Similar effects were observed in Mo–P–O glasses [14]. Surprisingly, very high values of density were obtained by annealing Mo–P–O glass of 40 mol % MoO_3. But nothing has

TABLE V Data for annealing effect on Mo–P–O glasses

Glass no.	MoO_3 (mol %)	Annealing temp. (K)	Density ($g\,cm^{-3}$)	Molar volume (cm^3)	Ultrasonic wave velocity ($m\,sec^{-1}$)		Elastic moduli (kbar)				Poisson's ratio	Debye temp. (K)
					Long.	Shear	Long.	Shear	Bulk	Young's		
A/7	40.0	473	2.738	52.1	4180	2460	478	166	257	410	0.235	330
		523	2.744	52.0	4183	2460	480	166	259	410	0.236	330
		573	2.752	51.9	4188	2462	483	167	260	413	0.236	330
		623	2.772	51.5	4196	2464	488	168	264	415	0.236	332
		673	2.798	51.0	4206	2470	495	171	267	423	0.237	333
		723	2.832	50.4	4220	2479	504	174	272	430	0.236	336
A/15	50.0	473	2.906	49.2	4356	2608	551	197	288	481	0.221	349
		523	2.918	49.0	4358	2610	554	199	289	486	0.220	350
		573	2.926	48.8	4360	2610	556	199	291	486	0.221	351
		623	2.942	48.6	4364	2614	560	201	292	490	0.220	352
		673	2.968	48.2	4372	2619	567	204	295	498	0.220	352
		723	2.996	47.7	4382	2625	575	206	300	503	0.220	355
		773	3.024	47.3	4399	2637	585	210	305	512	0.219	358
A/41	76.0	473	3.252	44.1	3978	2348	516	179	277	441	0.233	311
		523	3.258	44.0	3980	2351	516	180	276	443	0.232	312
	573	573	3.274	43.8	3985	2352	520	181	279	446	0.233	312
		613	3.301	43.4	3997	2358	527	182	284	449	0.233	314
		653	3.358	42.7	4017	2367	542	188	291	464	0.234	317

been reported elsewhere on the effect of annealing temperature on the elastic properties of these Mo–P–O glasses.

Three different Mo–P–O glasses of different compositions were studied at different annealing temperatures (see Table V). Most of the stresses caused during the casting were relieved, and the most suitable temperature, for this purpose, was a few degrees below transition temperature. The elastic moduli as well as density increase with the annealing temperature (see Figs. 18 to 21), but there is no observed change in the value of Poission's ratio of these glasses. The change in density of about 4% found in this series was much lower than that compared with the same series studied by Hekmat [15]. From the elastic moduli and density one can infer that annealing the glasses causes a slight reduction in average interatomic spacing so that the r^2f term in K_{bc} increases slightly (given that f varies as r^{-3}). Even with no structural changes, the reduced spacing will also cause the numbers of network bonds per unit volume, to increase. Thus, K_{bc} and therefore K_e increase, and so do all other moduli, since Poisson's

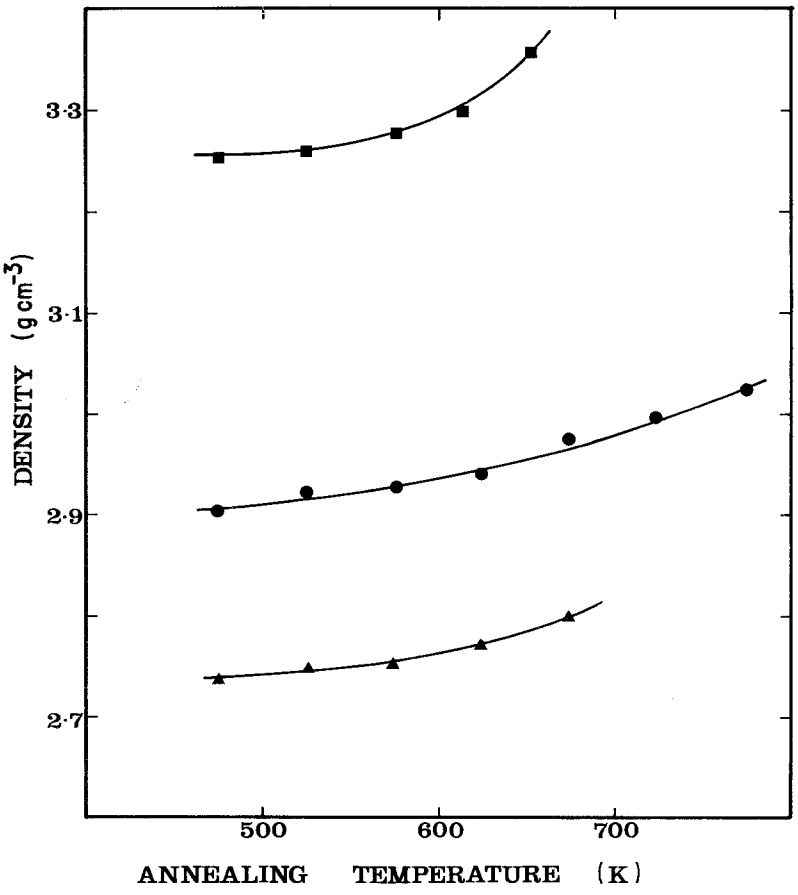

Figure 18 The effect of the annealing temperature on the density in Mo–P–O glasses.

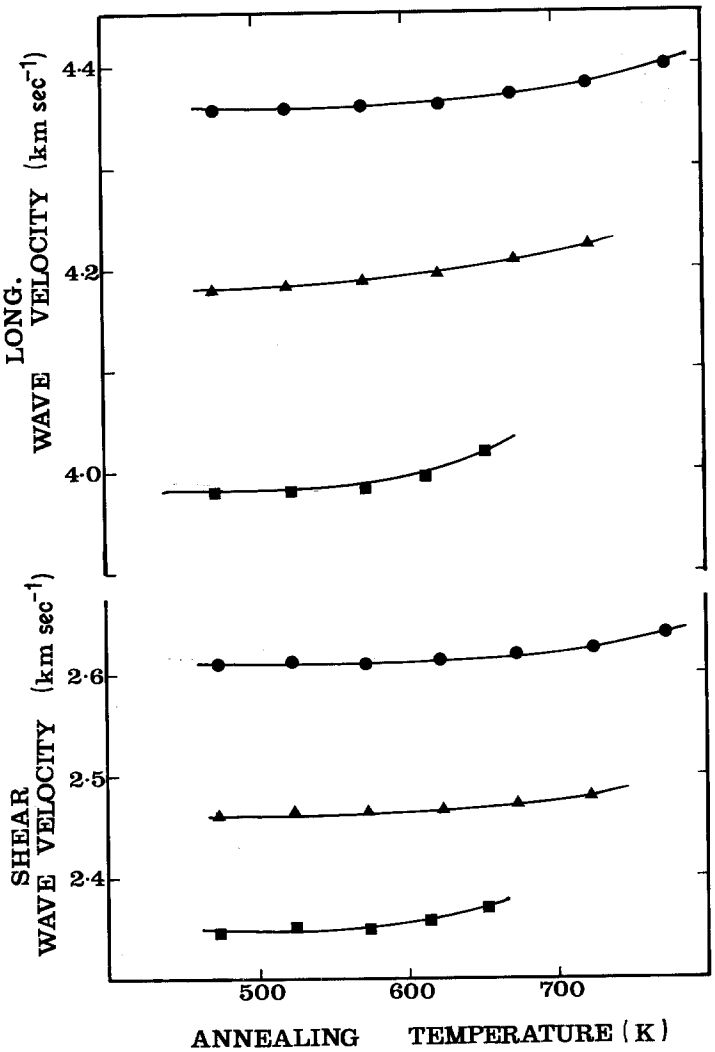

Figure 19 The effect of the annealing temperature on the ultrasound velocities in Mo–P–O glasses.

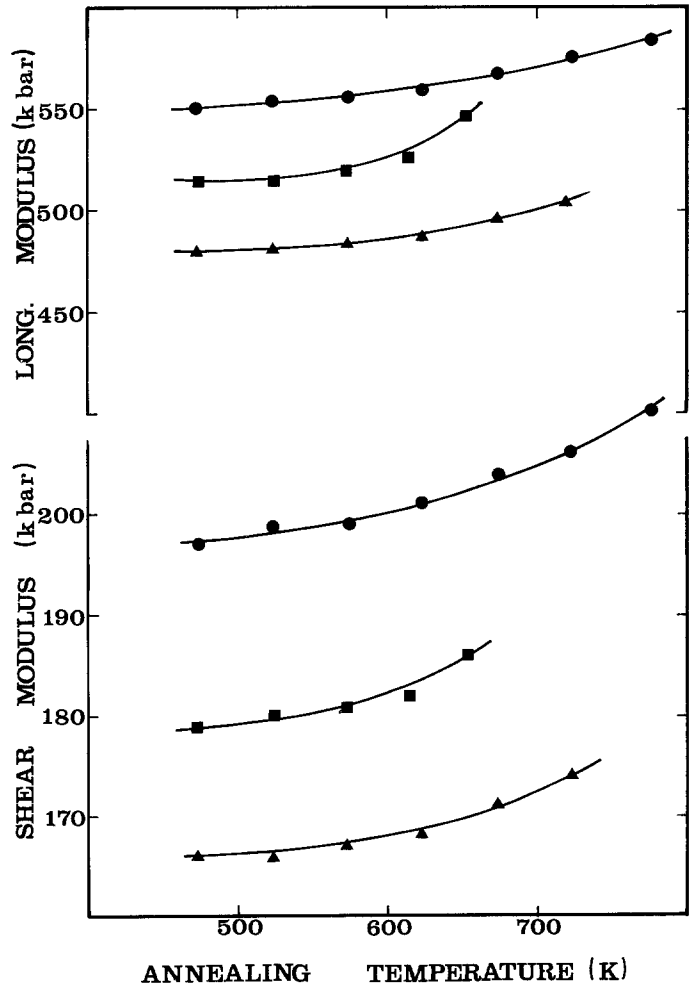

Figure 20 The effect of the annealing temperature on the longitudinal and shear modulus of the vitreous system MoO_3–P_2O_5.

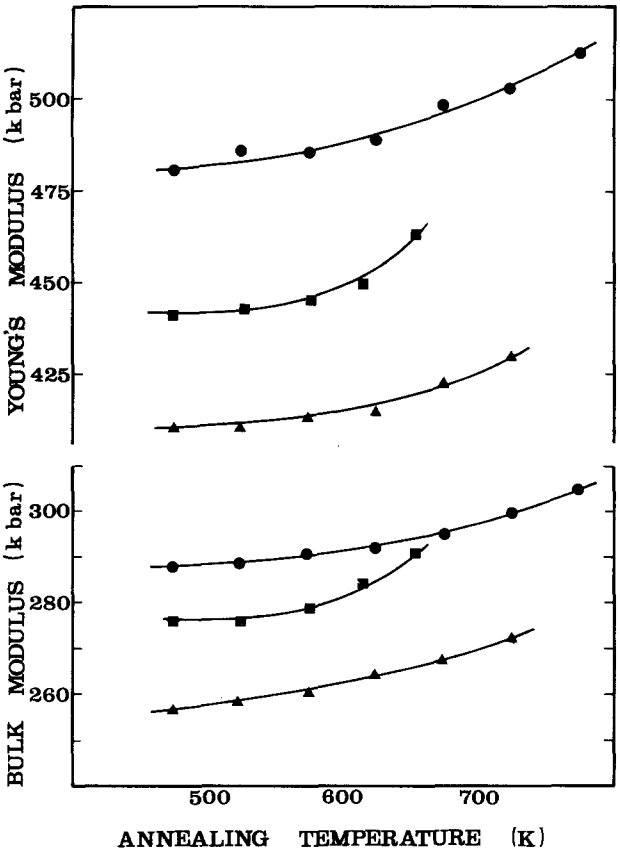

Figure 21 Dependence of the bulk and Young's modulus on annealing temperature for Mo–P–O glasses.

ratio stays constant. The latter is indicative of no changes in crosslink density per cation, i.e. essentially no structure rearrangements, during annealing.

12. Conclusions

Whilst elastic moduli data for glasses are numerous in the literature, systematic studies of how these properties vary with gradual composition changes over wide ranges, are relatively rare. In the present study of the complete Mo–P–O glass system, ultrasonically determined elastic moduli have been found to display discontinuities in their compositional gradients, at glass compositions approximating to metaphosphate and pyrophosphate. This is an interesting result given that density and molar volume vary monotonically with composition. It suggests that elastic moduli are especially sensitive indicators of structural changes in phosphate glasses. Given that direct structural data such as EXAFS measurements on this complete glass system (and for that matter on other complete phosphate glass systems) are not yet available, the ultrasonic exercise has yielded new information. Similar measurements on other binary vitreous phosphate glasses seem well worthwhile attempting. The composition dependence of the moduli has been qualitatively explained in terms of atomic ring sizes (and such force constant data as are available) on the assumption that the glasses consist of mixtures of metaphosphate, pyrophosphate, orthophosphate, MoO_3 and P_2O_5 groupings, in proportions that are a unique function of the glass composition $x Mo_2O_5\, y MoO_3 (1 - x - y) P_2O_5$. Of course a single glass system provides insufficient data to verify conclusively a qualitative theory of this kind. Data on a number of other phosphate glass systems will be required to put the theory to an adequate test, and the acquisition of such data may enable a more quantative interpretation to be developed.

References

1. N. D. PATEL and B. BRIDGE, *Phys. Chem. Glasses* **24** (1983) 130.
2. I. J. SCHULZ, *Anorg. Allgem. Chem.* **99** (1955) 281.
3. P. L. BAYNTON, H. RAWSON and J. E. STANWORTH, *Nature* **178** (1956) 910.
4. P. KIERKEGAARD, K. EISTRAT, and A. R. ROSENHALL, *Acta. Chem. Scand.* **18** (1964) 2237.
5. D. L. KEPERT, "The Early Transition Metals" (Academic, London, New York, 1972) pp. 255–368.
6. A. J. VOGEL, "Text book of Macro and Semi-micro quantitative Inorganic Analysis", 5th Edn. (Longman, London, New York, 1979) p. 511.
7. P. KIERKEGAARD, *Acta. Chem. Scand.* **12** (1958) 1701.
8. *Idem, Arkiv. Kemi.* **18** (1962) 521.
9. *Idem, ibid.* **19** (1962) 1.
10. P. KIERKEGAARD and M. WESTERLUND, *Acta. Chem. Scand.* **18** (1964) 2217.
11. D. N. WELLS, "Structural Inorganic Chemistry", 4th Edn. (Clarendon Press, Oxford, 1975).
12. A. MANSINGH, J. K. VAID and R. P. TANDON, *J. Phys.* **C8** (1975) 1023.
13. A. RASHID, PhD thesis, Brunel University (1980).
14. M. H. HEKMAT-SHOAR, PhD thesis, Brunel University (1979).
15. E. KORDES, *Z. Phys. Chem.* **50** (1950) 194.
16. B. BRIDGE and G. R. MORIDI, Proceedings of the Institute of Acoustics, Spring Conference and Exhibition, University of Bath, 4–6 April 1977, p6–4–1.
17. B. BRIDGE, N. D. PATEL and D. N. WATERS, *Phys. Status Solidi (a)* **77** (1983) 655.
18. G. R. MORIDI, PhD thesis, Brunel University (1975).
19. G. R. MORIDI and C. A. HOGARTH, *Int. J. Electron.* **54** (1983) 169.

Received 8 February
and accepted 30 May 1985